Johann Wolfgang von Goethe-Universität

Master Thesis

Twisted Mass Lattice Quantum Chromodynamics computations for B mesons and an outlook on $\bar{b}\bar{b}ud$ four-quark systems

---

Author:
Janik Kämper

Supervisor and first examiner:
Prof. Marc Wagner
Second examiner:
Prof. Pedro Bicudo

A thesis submitted in fulfilment of the requirements for the degree of Master of Science in Physics

Institute for Theoretical Physics

August 8, 2019

Eigenständigkeitserklärung

gemäß § 30 (12) Ordnung für den Bachelor - und Masterstudiengang

Hiermit erkläre ich, dass ich die Arbeit selbstständig und ohne Benutzung anderer als der angegebenen Quellen und Hilfsmittel verfasst habe. Alle Stellen der Arbeit, die wörtlich oder sinngemäß aus Veröffentlichungen oder aus anderen fremden Texten entnommen wurden, sind von mir als solche kenntlich gemacht worden. Ferner erkläre ich, dass die Arbeit nicht - auch nicht auszugsweise - für eine andere Prüfung verwendet wurde.

Frankfurt am Main, 08. August 2019

Abstract

In this thesis we give an introduction to Twisted Mass Quantum Chromodynamics and an actual implementation for the computations of effective masses for $\bar{b}q$ mesons in the static-light approximation with q being either a u or a d quark. We discuss the corresponding trial states creating the states with the desired quantum numbers on the lattice and the effective masses obtained from the simulation with unphysically heavy light quarks as well as the extrapolation of the effective masses in terms of the physical light quark mass. The other subject is are four-quark systems $\bar{b}\bar{b}ud$ and their theoretical description in terms of possible four-quark structures, i.e. mesonic molecule and the diquark-antidiquark state. Moreover, we give an approach for the implementation of the latter on the lattice.

Contents

Chapter 1

Introduction

Hadrons are compound particles based on quarks which are fundamental building bricks for all the matter surrounding us. After the discovery of hundreds of hadrons in the 1950s in particle experiments with newly invented detectors the question arose whether there is a framework to describe the sheer number of hadrons in a more elemental form. This lead to the discovery of the Standard Model of Particle Physics and the theory describing the strong interaction between quarks, Quantum Chromodynamics (QCD). Since then, the whole area of particle physics has been subject to investigations around the world. Hadrons occur either as baryons which are particles consisting of three quarks or as mesons consisting of a quark and an antiquark. Since computer power has been increased over time, those particles became subject to simulations until today.

We are especially concentrating on the computation of meson masses from Lattice QCD, a discretized version of continuum QCD to be carried out on computers. As time went by new methods and more powerful hardware has been explored, steadily leading to more precise results allowing for better comparisons with experimental data.

In this thesis we will concentrate on the Twisted Mass QCD which is an equivalent formulation of QCD with computational advantages when it is used in its lattice version. Therefore, we will give an introduction to this framework hand in hand with the computation of effective masses of certain mesons, i.e. mesons consisting of a heavy antiquark $\bar{b}$ and a light quark u or d building a bound state $\bar{b}u$ or $\bar{b}d$. Therefore, we will describe the mesons in terms of their quantum numbers and symmetries which is fundamental to relate the mesons with the states of the same structure created in the simulation. Moreover, we will accompany this procedure with technical aspects necessary to compute the quantities of interest.

Another part of this thesis deals with BB systems consisting of two antiquarks $\bar{b}\bar{b}$ and two light quarks ud building an exotic four-quark state $\bar{b}\bar{b}ud$ which are theoretically allowed to exist in nature but have only recently been discovered in experiments. Therefore, these are subject to recent studies in theoretical frameworks as well. B mesons and BB mesons are treated by similar means on the lattice and while we

will concentrate on the computation of effective masses for B mesons, we will give an introduction to BB systems and their different structures with regard to four-quark system, namely the mesonic molecule and the diquark-antidiquark state, respectivley. Furthermore, we will discuss their quantum numbers and symmetries and give an approach to an implementation for lattice computations.

Chapter 2

Theoretical background

2.1 Notations and conventions

We will often use expressions like $\psi_A^{a(f)}(x)$, where indices are explicit given. Greek lower case letters represent light quark or antiquark fields which usually have a colour index a denoted by lower case Latin letters with values in $\{1,2,3\}$, a spin index A denoted by upper case Latin letters with values in $\{0,1,2,3\}$ and a flavour index denoted either by an embraced flavour f or directly by replacing the quark field ψ by the flavour, i.e. u or d. Moreover, x denotes the four-dimensional spacetime point of the given quark field, which can also be written as $(\mathbf{x}, t)$, where $\mathbf{x}$ denotes a three-dimensional spatial point and $t \equiv x_0$ the time.

We use the chiral representation of the gamma matrices:

$$\gamma_0 = \begin{pmatrix} 0 & -\mathbb{1}_2 \\ -\mathbb{1}_2 & 0 \end{pmatrix}, \quad \gamma_j = \begin{pmatrix} 0 & +\sigma^j \\ -\sigma^j & 0 \end{pmatrix}$$

with the Pauli matrices

$$\tau^1 = \begin{pmatrix} 0 & +1 \\ +1 & 0 \end{pmatrix}, \quad \tau^2 = \begin{pmatrix} 0 & -i \\ +i & 0 \end{pmatrix}, \quad \tau^3 = \begin{pmatrix} +1 & 0 \\ 0 & -1 \end{pmatrix}.$$

2.2 Correlation functions

To get a trial state $|\psi\rangle$ with specific quantum numbers $I(J^P)$, these states have to be created. Therefore a so called creation operator $\mathcal{O}$ which creates these quantum numbers by acting on the QCD vacuum $|\Omega\rangle$

$$|\psi\rangle = \mathcal{O}\,|\Omega\rangle \tag{2.1}$$

needs to be built. A central quantity of all lattice computations are so called correlation functions which consist of creation operators introduced above [1], [2].

$$\begin{aligned} C(t) &\equiv \langle\Omega|\, \mathcal{O}^\dagger(t)\mathcal{O}(0)\, |\Omega\rangle \\ &= \sum_{n=0}^{\infty} \langle\Omega|\, e^{+Ht}\mathcal{O}^\dagger(0)e^{-Ht}\, |n\rangle\, \langle n|\, \mathcal{O}(0)\, |\Omega\rangle \\ &= \sum_{n=0}^{\infty} \underbrace{|\langle n|\, \mathcal{O}\, |\Omega\rangle|^2}_{=|a_n|^2} \exp(-\underbrace{(E_n - E_\Omega)}_{=m_n} t) \overset{t\gg 1}{\approx} |a_0|^2\, e^{-m_0 t} \end{aligned} \tag{2.2}$$

These correlation functions are then used to determine the effective masses of systems corresponding to the quantum numbers the creation operator implemented

$$m_{\text{eff}}(t) \equiv \frac{1}{a} \ln\left(\frac{C(t)}{C(t+a)}\right) \overset{t\gg 1}{\approx} m. \tag{2.3}$$

Since we are usually interested in computing potentials, $m_{\text{eff}}(t)$ can be computed for different separations of the two considered states. This procedure allows to obtain the potential as a function of the separation.

2.3 $N_f = 2$ twisted mass QCD

In this section we want to introduce the so called twisted mass QCD which is an equivalent formulation of QCD with modifications allowing for an improvement of discretization errors in its lattice version, see [3], [4], [5].

The continuum version of the twisted mass QCD action for $N_f = 2$ degenerate light quarks, i.e. the doublet $\chi = (\chi^{(u)}, \chi^{(d)})$, reads as follows

$$S_{light}[\chi, \bar{\chi}, A] = \int d^4x\, \bar{\chi}\left(\gamma_\mu D_\mu + m_q + i\mu_q\gamma_5\sigma^3\right)\chi, \tag{2.4}$$

where $\{\chi, \bar{\chi}\}$ denotes the set of fermion fields in the twisted basis, $D_\mu = \delta_\mu + A_\mu$ the covariant derivative for a given gauge field A_μ and m_q the untwisted quark mass. Moreover, μ_q denotes the twisted quark mass and σ^3 the third Pauli-matrix acting in flavour space.
In contrast to the twisted basis, the *physical basis* $\{\psi, \bar{\psi}\}$ denotes the basis for the standard QCD action. These two bases are related by a so called *twist rotation*

$$\psi = e^{i\frac{\omega}{2}\gamma_5\sigma^3}\chi, \quad \bar{\psi} = \bar{\chi}e^{i\frac{\omega}{2}\gamma_5\sigma^3}. \tag{2.5}$$

where ω denotes the so called *twist angle* which is a free parameter. With these transformations the form of the QCD action remains the same, but the mass term

undergoes a rotation. If we rewrite the mass term in (2.4)

$$m_q + i\mu_q\gamma_5\sigma^3 = Me^{i\alpha\gamma_5\sigma^3} \tag{2.6}$$

with the absolute value

$$M = \sqrt{m_q^2 + \mu_q^2} \tag{2.7}$$

and the angle α in the complex plain, we can see the twisted mass rotation directly:

$$Me^{i(\alpha-\omega)\gamma_5\sigma^3}. \tag{2.8}$$

That is, we obtain the standard QCD action for $\alpha = \omega$, i.e. if the twist angle ω fulfils

$$\tan\omega = \mu_q/m_q. \tag{2.9}$$

It can be shown that the so called automatic $\mathcal{O}(a)$ improvement is achieved at the maximal twist with $\omega = \pi/2$. For a deeper understanding, it is worth reading [3].

2.4 B mesons

In this thesis we want to concentrate on B mesons. These are mesons consisting of a $\bar{b}$ antiquark and a lighter quark q, while its counterpart, the $\bar{B}$ meson, consists of a b quark and a lighter antiquark $\bar{q}$. In our case, the light quark is either a u or a d quark. A star $*$ indicates mesons which have an even angular momentum quantum number and positive parity, i.e. $J^{\mathcal{P}} = 0^+, 2^+, ...$ as well as those which have an odd angular momentum quantum number and negative parity, i.e. $J^{\mathcal{P}} = 1^-, 3^-, ...$ [6].

2.4.1 Static light mesons

One way to investigate B mesons is to use the so called *Heavy Quark Effective Theory* (HQET). With this approach, the leading term is the static approximation. Due to the much higher mass of the b quark in comparison to the light quark, the b quark is treated as a static quark, i.e. as a particle with infinite mass and therefore with a fixed position in space while the light quark is treated dynamically, i.e. with a finite mass. This system is called a *static light meson*.

2.4.2 Quantum numbers and symmetries

In the following we will give an overview and some information over the possible quantum numbers involved in characterizing the B meson state.

Parity The first quantum number our system can be described with is parity. It can either be positive or negative, i.e. $P \in \{+, -\}$.

Isospin Since the static light meson consists of a u/d quark, its isospin is $I = 1/2$ and the z-component $I_z \in \{-1/2, +1/2\}$.

Angular momentum Moreover, the static quark spin does not affect the interaction of our B mesons which are in turn degenerate. Consequently, our system can be described by the total angular momentum corresponding to its light degrees of freedom. The total angular momentum is $j = |l \pm 1/2|$, where l is the orbital angular momentum which also includes the gluonic spin and $\pm 1/2$ is the spin of the light quark.

2.4.3 Meson creation operators and trial states

The notation for static light mesons is $\bar{Q}q$ and the trial states we are interested in, have the following structure

$$\bar{Q}\,\Gamma\,\psi\,|\Omega\rangle\,, \tag{2.10}$$

where Q denotes the heavy quark field and ψ the light quark field, respectively. Γ stands for an appropriate combination of γ-matrices describing the spin structure of our trial state.

For now, we are interested in the B meson ground state which is also referred to as S meson, and the first excited state, called P_- meson, respectively. The S state is characterized by orbital angular momentum $l = 0$ from which follows that its total angular momentum is $|j| = |j_z| = \frac{1}{2}$ as mentioned above. On top, it is the state with negative parity, i.e. $\mathcal{P} = -$. Since the spin of the heavy quark does not contribute to the interaction of the system, there are two corresponding states, i.e. $J^{\mathcal{P}} = 0^-$ or $J^{\mathcal{P}} = 1^-$. The same holds for the P_- state (same orbital/total angular momentum) except for the parity which is positive in that case, i.e. $J^{\mathcal{P}} = 0^+$ or $J^{\mathcal{P}} = 1^+$ corresponds to the P_-. The Γ structure we will consider is $\Gamma \in \{\mathbb{1}, \gamma_5\}$ for the $J^P = 0^+$ and the $J^P = 0^-$ state respectively.

In this thesis we will not discuss states with $l \neq 0$, i.e. states with excited orbital angular momentum. These states are described by other γ-combinations in the trial state.

2.4.4 Correlator

The next step on our agenda is to derive the correlator from our trial states for the purpose pointed out in section 2.2. This is of great importance, because these correlators are a crucial part in the actual code implementation for calculating effective masses. First, we write down the spin and colour indices in (2.10) explicitly. Then, the operator included in the trial state reads

$$\mathcal{O}(t) = \bar{Q}^a_A(t)\;\Gamma^t_{AB}\;\psi^a_B(t). \tag{2.11}$$

Note that Γ has no time dependence. The index indicates to which operator the matrix belongs to.

$$\begin{aligned}
C(t) &= \langle\Omega|\, \mathcal{O}^\dagger(t)\mathcal{O}(0)\,|\Omega\rangle \\
&= \langle\Omega|\, \left(\bar{Q}^a_A(t)\ \Gamma^t_{AB}\ q^a_B(t)\right)^\dagger\ \bar{Q}^b_C(0)\ \Gamma^0_{CD}\ q^b_D(0)\,|\Omega\rangle \\
&= \langle\Omega|\, \bar{q}^a_B(t)\ (\gamma_0\Gamma^{t,\dagger}\gamma_0)_{BA}\ Q^a_A(t)\ \bar{Q}^b_C(0)\ \Gamma^0_{CD}\ q^b_D(0)\,|\Omega\rangle \\
&= \langle\Omega|\, \bar{q}^a_B(t)\ \left(\gamma_0\Gamma^{t,\dagger}\gamma_0\right)_{BA}\Gamma^0_{CD}\ Q^a_A(t)\ \bar{Q}^b_C(0)\ q^b_D(0)\,|\Omega\rangle \\
&= -\langle\Omega|\, \left(\gamma_0\Gamma^{t,\dagger}\gamma_0\right)_{BA} Q^a_A(t)\ \bar{Q}^b_C(0)\ \Gamma^0_{CD}\ q^b_D(0)\ \bar{q}^a_B(t)\,|\Omega\rangle \\
&= -\left\langle \left(\gamma_0\Gamma^{t,\dagger}\gamma_0\right)_{BA} (\mathcal{Q}^{-1})^{ab}_{AC}(t,0)\ \Gamma^0_{CD}\ (\mathcal{D}^{-1})^{ba}_{DB}(0,t)\right\rangle \\
&= -e^{-Mt}\left\langle \left(\gamma_0\Gamma^{t,\dagger}\gamma_0\right)_{BA} U^{ab}(t,0)\left(\frac{1+\gamma_0}{2}\right)_{AC}\Gamma^0_{CD}\ (\mathcal{D}^{-1})^{ba}_{DB}(0,t)\right\rangle \\
&= -\frac{1}{2}e^{-Mt}\left\langle U^{ab}(t,0)\left(\gamma_0\Gamma^{t,\dagger}\gamma_0\right)_{BA}(1+\gamma_0)_{AC}\Gamma^0_{CD}(\mathcal{D}^{-1})^{ba}_{DB}(0,t)\right\rangle \\
&= -\frac{1}{2}e^{-Mt}\left\langle Tr_{spin}\left[U^{ab}(t,0)\left(\gamma_0\Gamma^{t,\dagger}\gamma_0\right)(1+\gamma_0)\Gamma^0(\mathcal{D}^{-1})^{ba}(0,t)\right]\right\rangle \\
&= -\frac{1}{2}e^{-Mt}\left\langle Tr\left[U(t,0)\left(\gamma_0\Gamma^{t,\dagger}\gamma_0\right)(1+\gamma_0)\Gamma^0\mathcal{D}^{-1}(0,t)\right]\right\rangle
\end{aligned} \tag{2.12}$$

After inserting the propagator according to stochastic timeslice sources (3.19), the correlator becomes

$$= -\frac{1}{2N}e^{-Mt}\left\langle \xi[n,t](0)^\dagger U(t,0)\left(\gamma_0\Gamma^{t,\dagger}\gamma_0\right)(1+\gamma_0)\Gamma^0\phi[n,t](t)\right\rangle \tag{2.13}$$

A more comprehensive version in vector matrix notation better suited for this case can be found in appendix A. In favour of further investigations with BB mesons, which have more complex correlators, explicit indices are shown to focus on corresponding structures. Here, $\langle\ldots\rangle$ denotes a path integral and $(\mathcal{Q}^{-1})^{ab}_{AC}(t,0)$ the heavy quark propagator (2.14) derived from Heavy Quark Effective Theory [7], [8].

$$\begin{aligned}
(\mathcal{Q}^{-1})^{ab}_{AC}(x;y) = \delta(x-y)U^{ab}(x,x_0;y,y_0)\Bigg(&\Theta(y_0-x_0)\left(\frac{1-\gamma_0}{2}\right)_{AC}\exp^{-M(y_0-x_0)} \\
&+\Theta(x_0-y_0)\left(\frac{1+\gamma_0}{2}\right)_{AC}\exp^{-M(x_0-y_0)}\Bigg)
\end{aligned} \tag{2.14}$$

2.4.5 Relation between physical and twisted basis

Since the whole calculation is carried out within the scope of twisted mass lattice QCD as pointed out in section 2.3, we have to transform the correlation functions after our calculation back from the twisted basis into the desired physical basis according to (2.5). Therefore, we use the mentioned equations with the maximal twist $\omega = \pi/2$.

This results in the following specific transformation equations for the fermion fields

$$\psi^{(u)} = \frac{1}{\sqrt{2}}(\mathbb{1} + i\gamma_5)\chi^{(u)} \qquad \bar{\psi}^{(u)} = \bar{\chi}^{(u)}\frac{1}{\sqrt{2}}(\mathbb{1} + i\gamma_5), \tag{2.15}$$

$$\psi^{(d)} = \frac{1}{\sqrt{2}}(\mathbb{1} - i\gamma_5)\chi^{(d)} \qquad \bar{\psi}^{(d)} = \bar{\chi}^{(d)}\frac{1}{\sqrt{2}}(\mathbb{1} - i\gamma_5), \tag{2.16}$$

which only differ by a relative minus sign due to the rotation regarding the third Pauli-matrix in (2.5) corresponding to the two flavours u and d.

The overall Γ-matrix of the correlation function given in (2.12) has the general form

$$\Gamma = \Gamma_t(\mathbb{1} + \gamma_0)\Gamma_0. \tag{2.17}$$

As a result, we are able to calculate this Γ-matrix in dependence of Γ^t and Γ^0 with regard to the twisted basis. In order to do so, we simply have to insert the γ-matrices corresponding to the states we are interested in, since the calculation of the correlation function takes place in the twisted basis as mentioned above.

As an example we show the case for $\Gamma_t = \gamma_5$ and $\Gamma_0 = \mathbb{1}$.

Twisted basis:

$$\begin{aligned}\Gamma &= \gamma_0\Gamma_t^\dagger\gamma_0(\mathbb{1} + \gamma_0)\Gamma_0 \\ &= -\gamma_5(\mathbb{1} + \gamma_0)\mathbb{1} \\ &= -(\gamma_5 + \gamma_5\gamma_0) \\ &= -(\gamma_5 - \gamma_0\gamma_5) \\ &= \gamma_0\gamma_5 - \gamma_5\end{aligned} \tag{2.18}$$

To obtain the correlation function with regard to the physical basis, we have to express the operators in the physical basis in terms of the operators in the twisted basis. By means of the twist rotation with maximal twist (2.15) and (2.16) we get

$$\mathcal{O}_1^{tb} = \bar{Q}\chi = \bar{Q}\frac{1}{\sqrt{2}}\left(\mathbb{1} \mp i\gamma_5\right)\psi = \frac{1}{\sqrt{2}}\Big(\underbrace{\bar{Q}\psi}_{\mathcal{O}_1^{pb}} \mp i\underbrace{\bar{Q}\gamma_5\psi}_{\mathcal{O}_5^{pb}}\Big) = \frac{1}{\sqrt{2}}\Big(\mathcal{O}_1^{pb} \mp i\mathcal{O}_5^{pb}\Big), \tag{2.19}$$

$$\mathcal{O}_5^{tb} = \bar{Q}\gamma_5\chi = \bar{Q}\gamma_5\frac{1}{\sqrt{2}}(\mathbb{1} \mp i\gamma_5)\psi = \frac{1}{\sqrt{2}}\Big(\underbrace{\bar{Q}\gamma_5\psi}_{\mathcal{O}_5^{pb}} \mp i\underbrace{\bar{Q}\psi}_{\mathcal{O}_1^{pb}}\Big) = \frac{1}{\sqrt{2}}\Big(\mathcal{O}_5^{pb} \mp i\mathcal{O}_1^{pb}\Big), \tag{2.20}$$

and thus, can express the operators in the physical basis in terms of linear combinations of operators in the twisted basis

$$\mathcal{O}_1^{pb} = \frac{1}{\sqrt{2}}(\mathcal{O}_1^{tb} \pm i\mathcal{O}_5^{tb}) \tag{2.21}$$

$$\mathcal{O}_5^{pb} = \frac{1}{\sqrt{2}}(\mathcal{O}_5^{tb} \pm i\mathcal{O}_1^{tb}) \tag{2.22}$$

In order to build up the correlation matrix in the physical basis, we express each correlation function in the physical basis C^{pb} in terms of the correlation functions in the twisted basis C^{tb}. For a better readability the angular brackets were dropped. For the case we dealt with above, this reads as follows:

$$\begin{aligned} C_{51}^{pb} &= \left(\mathcal{O}_5^{pb}\right)^\dagger \mathcal{O}_1^{pb} \\ &= \frac{1}{\sqrt{2}}\left(\left(\mathcal{O}_5^{tb}\right)^\dagger \mp i\left(\mathcal{O}_1^{tb}\right)^\dagger\right)\frac{1}{\sqrt{2}}\left(\mathcal{O}_1^{tb} \pm i\mathcal{O}_5^{tb}\right) \\ &= \frac{1}{2}\left(\left(\mathcal{O}_5^{tb}\right)^\dagger \mathcal{O}_1^{tb} \mp i\left(\mathcal{O}_1^{tb}\right)^\dagger \mathcal{O}_1^{tb} \pm i\left(\mathcal{O}_5^{tb}\right)^\dagger \mathcal{O}_5^{tb} + \left(\mathcal{O}_1^{tb}\right)^\dagger \mathcal{O}_5^{tb}\right) \\ &= \frac{1}{2}\left(C_{51}^{tb} \mp iC_{11}^{tb} \pm iC_{55}^{tb} + C_{15}^{tb}\right). \end{aligned}$$

Considering only the Γ-matrix structure and account for the linearity of the correlator

$$\begin{aligned} &\widehat{=} \frac{1}{2}\left(\gamma_0\gamma_5 - \gamma_5 \mp i(\gamma_0 + \mathbb{1} - (\gamma_0 - \mathbb{1})) + \gamma_0\gamma_5 + \gamma_5\right) \\ &= \gamma_0\gamma_5 \mp i\mathbb{1} \end{aligned} \tag{2.23}$$

This procedure has to be repeated for all other γ-combinations regarding the states of interest. The other cases can be found in A.1. The results are listed in table 2.1.

Γ_t, Γ_0	Twisted basis	Physical basis
$\Gamma_t = \gamma_5, \Gamma_0 = \gamma_5$	$\gamma_0 - \mathbb{1}$	$\gamma_0 - i\gamma_5$
$\Gamma_t = \gamma_5, \Gamma_0 = \mathbb{1}$	$\gamma_0\gamma_5 - \gamma_5$	$\gamma_0\gamma_5 - i$
$\Gamma_t = \mathbb{1}, \Gamma_0 = \gamma_5$	$\gamma_0\gamma_5 + \gamma_5$	$\gamma_0\gamma_5 + i$
$\Gamma_t = \mathbb{1}, \Gamma_0 = \mathbb{1}$	$\gamma_0 + \mathbb{1}$	$\gamma_0 + i\gamma_5$

TABLE 2.1: Relation between twisted and physical basis

The usual strategy is to compute the correlation function for every occurring linear factor of the possible Γ-matrices shown in table 2.1. In this case we can - despite of the imaginary unit i - locate four γ-matrix combinations

$$\Gamma \in \{\mathbb{1}, \gamma_0, \gamma_5, \gamma_0\gamma_5\}. \tag{2.24}$$

2.5 BB systems

In this section we want to introduce four-quark states $\bar{b}\bar{b}qq$. These consist of two $\bar{b}$ quarks and two lighter quarks which can in principle have different flavours $q \in \{u, d, s, c\}$ depending on the system of interest. In our case we concentrate on u and d quarks. As in the case of B mesons, the heavy quarks can be treated with infinite mass and thus can be described in terms of the static approximation. These systems are essentially combinations of two static light mesons B to build up a four-quark system. In the following sections we will give information about BB systems in terms of quantum numbers and symmetries and their differences occurring when changing from continuum QCD to twisted mass lattice QCD.

2.5.1 Motivation

In principle, tetraquarks can be characterised by different structures. One possibility is to investigate four-quark systems $\bar{b}\bar{b}qq$ in terms of B mesons: Two B mesons, each consisting of a $\bar{b}$ quark and a lighter u or d quark, when bound together, can form a so called *mesonic molecule* which can be identified as tetraquark. Another possibility is a so called *diquark-antidiquark* which consists of the same quarks but contrary to the mesonic molecule, the heavy quarks $\bar{b}$ form an antidiquark while the lighter quarks qq form a diquark. A visualisation is shown in figure 2.1. In contrast to the B mesons, diquarks and antidiquarks are not colour singlets and thus can only occur in bound states, e.g. a $\bar{b}\bar{b}qq$ system. The overall aim of the computation is to obtain the

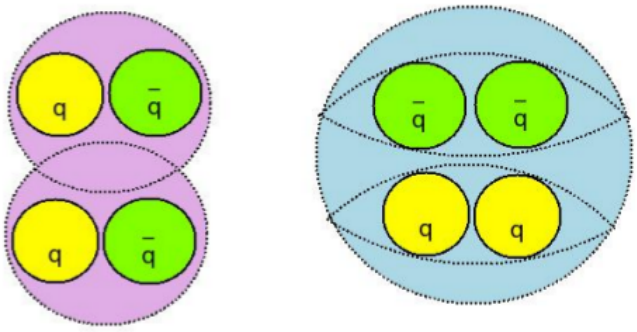

FIGURE 2.1: Two different structures for tetraquarks: On the left a drawing of the mesonic molecule and on the right a drawing of the diquark-antidiquark is shown. Taken from [6].

interaction of the two heavy quarks $\bar{b}\bar{b}$ in presence of the lighter quarks qq [9] with the purpose of finding candidates for bound four-quark states which can be identified as tetraquarks. This is done utilizing the so called *Born-Oppenheimer approximation* which was originally introduced in 1927 to separate the wave function of the electrons from the wave function of the nuclei of a molecule. This is possible due to the large mass difference of the electron and the nuclei mass, respectively. For a $\bar{b}\bar{b}qq$ system considered in the static approximation, this framework can also be applied since the

mass of the heavy quarks vastly exceeds the mass of the light quarks. The advantage is, that it paves the way for a better understanding of the binding of the four-quark state beyond the fact that bound states occur with certainty within in the scope of QCD if only the b quarks are heavy enough. The Born-Oppenheimer approximation allows to determine the wave function of the heavy quarks $\bar{b}\bar{b}$. This is done with regard to the potential of the heavy antiquarks in presence of the light quarks [6]. For small distances between the heavy antiquarks, these interact with a perturbative one-gluon-exchange Coulomb potential, while the interaction is screened by the light quarks for large distances between the heavy antiquarks as illustrated in figure 2.2. This leads to two weakly interacting B mesons [10]. With this approach the heavy

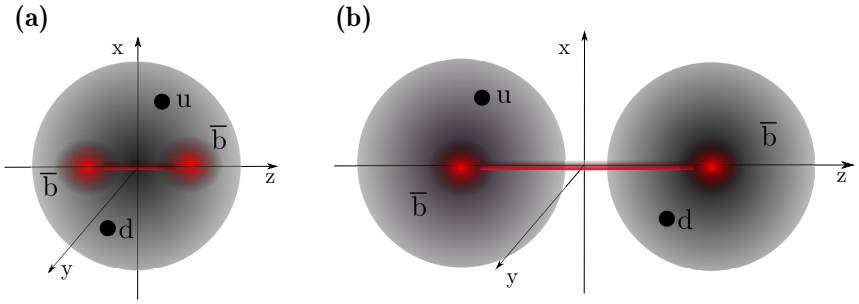

FIGURE 2.2: $\bar{b}\bar{b}qq$ system. (a) For short separations of $\bar{b}\bar{b}$, the heavy antiquarks interact with a perturbative one-gluon-exchange Coulomb potential. (b) For large separations, the interaction of the heavy antiquarks is screened by the light quarks. Taken from [10].

antiquarks $\bar{b}\bar{b}$ can be approximated as static colour charges with regard to the light quarks and thus we are able to obtain the energy of the light quarks from lattice QCD. In the second step, these energies can be used in return as the effective potential for the heavy antiquarks. If this potential is inserted into the Schrödinger equation and the energy eigenvalues are calculated, it is possible to state if the potential is able to lead to a bound system.

Recent studies, [11], [9], [10] investigated the potential of BB mesons for various states characterized by the quantum numbers discussed below leading to rules whether a potential is repulsive or attractive. Moreover, they show that there are four-quark systems which are candidates for bound $\bar{b}\bar{b}ud$ tetraquark states. These computations have in common that they made use of the mesonic molecule structure of tetraquarks. In order to better understand the interaction reaching from small to large separations of the heavy antiquarks $\bar{b}\bar{b}$, it is therefore desirable to carry out these computations within the scope of another tetraquark structure, i.e. the diquark-antidiquark structure and to compare the results with those obtained from the mesonic molecule structure.

2.5.2 Quantum numbers

In the following we will give an overview of the quantum numbers describing the $\bar{b}\bar{b}ud$ system. Since the heavy quarks are infinitely heavy, they have a fixed position. Since we want to extract the potential between those static light mesons as a function of their spatial separation r, we choose the positions of the static light mesons to be $\mathbf{r}_1 = (0, 0, -r/2)$ and $\mathbf{r}_2 = (0, 0, +r/2)$.

Parity For BB systems, parity is a quantum number and can be positive or negative, i.e. $\mathcal{P} \in \{+, -\}$.

Isospin As the BB system's isospin is only carried by its light quarks u and d, isospin can take values $I \in \{0, 1\}$ and its z-component $I_z \in \{-1, 0, 1\}$.

Angular momentum Since the heavy quarks are immobile and separated by r, rotations are only allowed around the axis of separation. Moreover, the static quarks' spin does not contribute to the interaction of the BB system and thus the the states can be labelled by the z-component of the angular momentum of the light degrees of freedom, i.e. $j_z \in \{-1, 0, 1\}$.

Reflection along the x-axis For $j_z = 0$ there exists a reflection around an arbitrary axis perpendicular to the axis of separation which is usually chosen to be the x-axis and denoted as $\mathcal{P}_x$. For states with $j_z \neq 0$, $\mathcal{P}_x \in \{+, -\}$ can be used as quantum number if we use $|j_z|$ instead.

Thus, the BB system can be described by five quantum numbers, $I, I_z, |j_z|, \mathcal{P} and \mathcal{P}_x$.

These quantum numbers are subject to symmetry breaking effects. First of all, the Wilson formulation of lattice QCD breaks some symmetries of the continuum version which are only restored in the continuum limit. On top of that, the twisted mass formulation of QCD has additional not exact symmetries, i.e. parity and isospin which will be restored in the continuum limit, too [3].

2.5.3 Diquark-Antidiquark

Now we want to introduce the trial states representing the diquark-antidiquark structure of the BB system. The overall trial state can be written in terms of the parts for the diquark and the antidiquark, i.e.

$$(C\Gamma)_{AB}\; u^b_A(\mathbf{z}, t)\; d^a_B(\mathbf{z}, t)\; \epsilon^{cab} \tag{2.25}$$

for the diquark and

$$\bar{Q}^f_C(\mathbf{x}, t)\; U^{fd}(\mathbf{x}, t; \mathbf{z}, t)\; \epsilon^{cde}\; \bar{Q}^g_{C'}(\mathbf{y}, t)\; U^{ge}(\mathbf{y}, t; \mathbf{z}, t) \tag{2.26}$$

for the antidiquark. With the charge conjugation matrix $\mathcal{C} = \gamma_0\gamma_2$ in correspondence to the chosen Gellmann matrices, see section 2.1, the trial states then read in summary

$$\begin{aligned}\mathcal{O} =&(C\Gamma)_{AB}\ (C\tilde{\Gamma})_{CC'} \\ &u^b_A(\mathbf{z},t)\ d^a_B(\mathbf{z},t)\ \epsilon^{cab}\ \bar{Q}^f_C(\mathbf{x},t)\ U^{fd}(\mathbf{x},t;\mathbf{z},t)\ \epsilon^{cde}\ \bar{Q}^g_{C'}(\mathbf{y},t)\ U^{ge}(\mathbf{y},t;\mathbf{z},t). \quad (2.27)\end{aligned}$$

The Levi-Civita symbols are introduced to account for the preservation of colour neutrality, i.e. that the diquark and the antidiquark are coupled to a colour singlet. Moreover, Γ and $\tilde{\Gamma}$ are as in the case of the B meson combinations of γ-matrices representing the spin structure. Although the heavy quarks' spin decouples from the system, we will keep it in the calculation and see that it will eventually drop out. A visualisation of the corresponding correlation function is shown in figure 2.3.

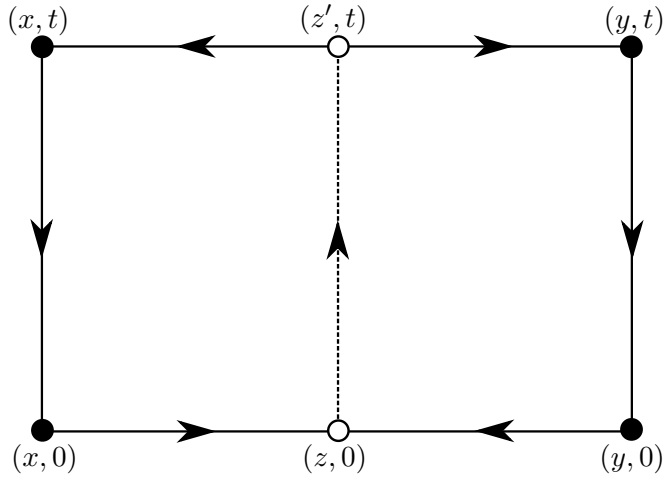

FIGURE 2.3: Diquark-Antidiquark

Now, we are able to calculate the correlation function $\mathcal{C}(t)$:

$$
\begin{aligned}
C &= \sum_{\mathbf{z}'} \langle \Omega | \mathcal{O}(t)^\dagger \mathcal{O}(0) | \Omega \rangle \\
&= \sum_{\mathbf{z}'} \langle \Omega | ((C\Gamma(t))_{AB}\ (C\tilde{\Gamma}(t))_{CC'}\ u^b_A(z',t)\ d^a_B(z',t)\ \epsilon^{cab} \\
&\quad \bar{Q}^f_C(x,t)\ U^{fd}(x,t;z',t)\ \epsilon^{cde}\ \bar{Q}^g_{C'}(y,t)\ U^{ge}(y,t;z',t))^\dagger \\
&\quad (C\Gamma(0))_{DE}\ (C\tilde{\Gamma}(0))_{FF'}\ u^i_D(y,0)\ d^k_E(z,0)\ \epsilon^{jki} \\
&\quad \bar{Q}^n_F(x,0)\ U^{nl}(x,0;z,0)\ \epsilon^{jlm}\ \bar{Q}^o_{F'}(y,0)\ U^{om}(y,0;z,0) | \Omega \rangle \\
&= \sum_{\mathbf{z}'} \langle \Omega | (\Gamma(t)^\dagger C^\dagger)_{BA}\ (\tilde{\Gamma}(t)^\dagger C^\dagger)_{C'C}\ \bar{u}^b_P(z',t)(\gamma_0)_{PA}\ \bar{d}^a_Q(z',t)(\gamma_0)_{QB}\ \epsilon^{cab} \\
&\quad (\gamma_0)_{CR} Q^f_R(x,t)\ U^{df}(x,t;z',t)\ \epsilon^{cde}\ (\gamma_0)_{C'S} Q^g_S(y,t)\ U^{eg}(y,t;z',t) \\
&\quad (C\Gamma(0))_{DE}\ (C\tilde{\Gamma}(0))_{FF'}\ u^i_D(z',0)\ d^k_E(z,0)\ \epsilon^{jki} \\
&\quad \bar{Q}^n_F(x,0)\ U^{nl}(x,0;z,0)\ \epsilon^{jlm}\ \bar{Q}^o_{F'}(y,0)\ U^{om}(y,0;z,0) | \Omega \rangle \\
&= \sum_{\mathbf{z}'} \langle \Omega | (\gamma_0 \Gamma(t)^\dagger C^\dagger \gamma_0)_{QP}\ (\gamma_0 \tilde{\Gamma}(t)^\dagger C^\dagger \gamma_0)_{SR}\ \bar{u}^b_P(z',t)\ \bar{d}^a_Q(z',t)\ \epsilon^{cab} \\
&\quad Q^f_R(x,t)\ U^{df}(x,t;z',t)\ \epsilon^{cde}\ Q^g_S(y,t)\ U^{eg}(y,t;z',t) \\
&\quad (C\Gamma(0))_{DE}\ (C\tilde{\Gamma}(0))_{FF'}\ u^i_D(z',0)\ d^k_E(z,0)\ \epsilon^{jki} \\
&\quad \bar{Q}^n_F(x,0)\ U^{nl}(x,0;z,0)\ \epsilon^{jlm}\ \bar{Q}^o_{F'}(y,0)\ U^{om}(y,0;z,0) | \Omega \rangle \\
&= \exp^{-2Mt} \sum_{\mathbf{z}'} (\gamma_0 \Gamma(t)^\dagger C^\dagger \gamma_0)_{QP}\ (C\Gamma(0))_{DE} \\
&\quad (\gamma_0 \tilde{\Gamma}(t)^\dagger C^\dagger \gamma_0)_{SR} \left(\frac{1+\gamma_0}{2}\right)_{RF} (C\tilde{\Gamma}(0))_{FF'} \left(\frac{1+\gamma_0}{2}\right)_{F'S} \\
&\quad \langle D^{-1ib}_{DP}(z,0;z',t)\ U^{df}(x,t;z',t)\ U^{fn}(x,t;x,0)\ U^{nl}(x,0;z,0)\ \epsilon^{cab}\ \epsilon^{cde}\ \epsilon^{jki}\ \epsilon^{jlm} \\
&\quad D^{-1ka}_{EQ}(z,0;z',t)\ U^{eg}(y,t;z',t)\ U^{go}(y,t;y,0)\ U^{om}(y,0;z,0) \rangle \\
&= -2 \exp^{-2Mt} \sum_{\mathbf{z}'} (\gamma_0 \Gamma(t)^\dagger C^\dagger \gamma_0)_{QP}\ (C\Gamma(0))_{DE} \\
&\quad \langle D^{-1ib}_{DP}(z,0;z',t)\ U^{df}(x,t;z',t)\ U^{fn}(x,t;x,0)\ U^{nl}(x,0;z,0)\ (\delta_{ad}\delta_{be} - \delta_{ae}\delta_{bd})(\delta_{kl}\delta_{im} - \delta_{km}\delta_{il}) \\
&\quad D^{-1ka}_{EQ}(z,0;z',t)\ U^{eg}(y,t;z',t)\ U^{go}(y,t;y,0)\ U^{om}(y,0;z,0) \rangle \\
&= -2 \exp^{-2Mt} \sum_{z'} \frac{1}{N^2} \sum_{n,m=1}^{N} (\gamma_0 \Gamma(t)^\dagger C^\dagger \gamma_0)_{QP}\ (C\Gamma(0))_{DE}\ \ (\delta_{ad}\delta_{be} - \delta_{ae}\delta_{bd})(\delta_{kl}\delta_{im} - \delta_{km}\delta_{il}) \\
&\quad \langle \phi[n,t]^{i(u)}_D(z,0)\ \phi[m,t]^{k(d)}_E(z,0)\ U^{df}(x,t;z',t)\ U^{fn}(x,t;x,0)\ U^{nl}(x,0;z,0) \\
&\quad \xi[m,t]^{a(d)}_Q(z',t)^\dagger\ \xi[n,t]^{b(u)}_P(z',t)^\dagger\ U^{eg}(y,t;z',t)\ U^{go}(y,t;y,0)\ U^{om}(y,0;z,0) \rangle
\end{aligned}
\tag{2.28}
$$

where we used

$$
(\gamma_0 \tilde{\Gamma}(t)^\dagger C^\dagger \gamma_0)_{SR} \left(\frac{1+\gamma_0}{2}\right)_{RF} (C\tilde{\Gamma}(0))_{FF'} \left(\frac{1+\gamma_0}{2}\right)_{F'S} = -2,
$$

inserted the quark propagator (3.19) and rewrote the Levi-Civita symbols in terms of Kronecker delta symbols for a more straightforward way to implement the correlator.

Moreover, we used the static quark propagator (2.14).

2.5.4 Mesonic molecule

For a comparison we will give a short overview of the trial states for mesonic molecules. Since one could further investigate the potential of $\bar{b}\bar{b}qq$ systems with a extended version of the mesonic molecule as illustrated in figure 2.4, it is not really necessary due to the applied Gaussian smearing causing the result to be indifferent.

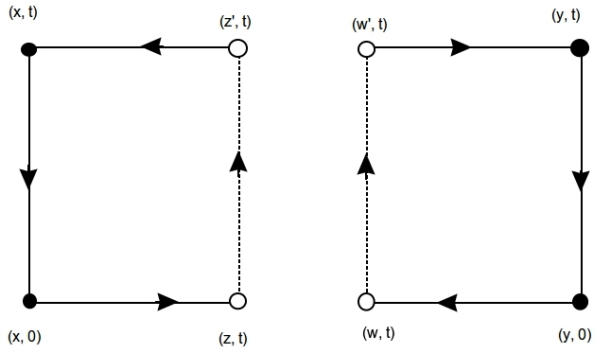

FIGURE 2.4: Extended Mesonic Molecule

Therefore, the usual correlator for mesonic molecules reads as follows:

$$\mathcal{O} = (C\Gamma)_{AB}\,(C\tilde{\Gamma})_{CC'}\,\bar{Q}^a_C(x,t)\,u^a_A(x,t)\,\bar{Q}^c_{C'}(y,t)\,d^c_B(y,t) \tag{2.29}$$

As mentioned above, $\mathcal{C} = \gamma_0\gamma_2$ is the charge conjugation matrix and Γ as well as $\tilde{\Gamma}$ are combinations of γ-matrices describing the spin structure. Note that in contrast to the trial states for the diquark-antidiquark (2.27), no Levi-Civita symbols are needed because both B mesons are already colour singlets.

Chapter 3

Technical aspects

In this chapter, we will discuss several techniques used in lattice QCD. These range from necessary implementations to improvements of statistical errors.

3.1 Lattice setup

First, we want to give an overview of the ensembles used for our lattice calculations.

Ensemble	β	lattice	κ	$a\mu$	m_π [MeV]	a [fm]
B40.24	3.9	$24^3 \times 48$	0.160856	0.0040	314	0.0855
B85.24	3.9	$24^3 \times 48$	0.160856	0.0085	448	0.0855
B150.24	3.9	$24^3 \times 48$	0.160856	0.0150	597	0.0855

TABLE 3.1: Ensembles and their parameters of $N_f = 2$ gauge configurations generated by the ETMC. The inverse bare coupling β, the lattice size measured in $(L/a)^3 \times (T/a)$, the bare light quark mass in lattice units $a\mu$, the pion mass m_π and the lattice spacing a are shown.

Since the pion masses are listed in 3.1 and are suitable for testing purposes, the correlator for the pion is given in appendix A.2.2.

3.2 Symmetry averaging

Symmetry averaging is a technique to achieve better statistics and to confirm the correctness of the computed contractions. The following symmetries are used for that purpose. Note that the symmetries for the quark fields in the twisted basis include a flavour exchange.

3.2.1 Symmetries

Parity $\mathcal{P}$

$$\begin{aligned} \psi(\mathbf{x}) &\xrightarrow{\mathcal{P}} \gamma_0 \psi(-\mathbf{x}) \\ \bar{\psi}(\mathbf{x}) &\xrightarrow{\mathcal{P}} \bar{\psi}(-\mathbf{x})\gamma_0 \end{aligned} \tag{3.1}$$

Twisted mass parity $\mathcal{P}^{tm}$

$$\begin{aligned} \chi^{(u)}(\mathbf{x}) &\xrightarrow{\mathcal{P}^{tm}} \gamma_0 \chi^{(d)}(-\mathbf{x}) \\ \bar{\chi}^{(u)}(\mathbf{x}) &\xrightarrow{\mathcal{P}^{tm}} \bar{\chi}^{(d)}(-\mathbf{x})\gamma_0 \end{aligned} \tag{3.2}$$

Charge conjugation $\mathcal{C}$

$$\begin{aligned} \psi &\xrightarrow{\mathcal{C}} \gamma_0\gamma_2\bar{\psi}^T \\ \bar{\psi} &\xrightarrow{\mathcal{C}} -\psi^T\gamma_2\gamma_0 \end{aligned} \tag{3.3}$$

Twisted mass time reversal $\mathcal{T}^{tm}$

$$\begin{aligned} \chi^{(u)}(\mathbf{x},t) &\xrightarrow{\mathcal{T}^{tm}} \gamma_0\gamma_5 \chi^{(d)}(\mathbf{x},-t) \\ \bar{\chi}^{(u)}(\mathbf{x},t) &\xrightarrow{\mathcal{T}^{tm}} \bar{\chi}^{(d)}(\mathbf{x},-t)\gamma_5\gamma_0 \end{aligned} \tag{3.4}$$

Twisted mass γ_5-hermiticity

$$\begin{aligned} \chi^{(u)} &\xrightarrow{\gamma_5^{tm}} \gamma_5 \chi^{(d)\dagger} \\ \bar{\chi}^{(u)} &\xrightarrow{\gamma_5^{tm}} \bar{\chi}^{(d)\dagger}\gamma_5 \end{aligned} \tag{3.5}$$

Subsequently we are able to derive rules which define how we have to combine the correlation functions with respect to the mentioned symmetries above and the occuring γ matrices in (2.24).

3.2.2 Symmetry transformation rules

The general spin structure only depends on the light degrees of freedom:

$$\left(\gamma_0\Gamma^{t,\dagger}\gamma_0\right)_{BA} (\mathbb{1}+\gamma_0)_{AC}\Gamma^0_{CD}\; q^b_D(0)\; \bar{q}^a_B(t) \tag{3.6}$$

Twisted mass time reversal $\mathcal{T}^{tm}$

$$\begin{aligned} &\left(\gamma_0\Gamma^{t,\dagger}\gamma_0\right)_{BA} (\mathbb{1}+\gamma_0)_{AC}\Gamma^0_{CD}\; q^b_D(0)\; \bar{q}^a_B(t) \\ &\xrightarrow{\mathcal{T}^{tm}} \left(\gamma_0\Gamma^{t,\dagger}\gamma_0\right)_{BA} (\mathbb{1}+\gamma_0)_{AC}\Gamma^0_{CD}\; (\gamma_0\gamma_5)_{DS} q^b_S(0)\; \bar{q}^a_T(-t)(\gamma_5\gamma_0)_{TB} \\ &= (\gamma_0\gamma_5)_{TB}\left(\gamma_0\Gamma^{t,\dagger}\gamma_0\right)_{BA} (\mathbb{1}+\gamma_0)_{AC}\Gamma^0_{CD}\; (\gamma_5\gamma_0)_{DS} q^b_S(0)\; \bar{q}^a_T(-t) \\ &= \left(\gamma_0\gamma_5\gamma_0\Gamma^{t,\dagger}\gamma_0(\mathbb{1}+\gamma_0)\Gamma^0\;\gamma_5\gamma_0\right)_{TS} q^b_S(0)\; \bar{q}^a_T(-t) \end{aligned} \tag{3.7}$$

Therefore, the rules we deduce are:

- Contractions computed in positive and negative time direction have to be merged, i.e. $+t \leftrightarrow -t$.
- Contractions with exchanged flavours have to be related, i.e. $u \leftrightarrow d$.

- Due to the additional γ matrices, there is a sign change according to $\Gamma \leftrightarrow \gamma_0\gamma_5\Gamma\gamma_5\gamma_0$, i.e. a sign change for $\Gamma \in \{\gamma_0, \gamma_5\}$.

Twisted mass parity $\mathcal{P}^{tm}$

$$\begin{aligned}
&\left(\gamma_0\Gamma^{t,\dagger}\gamma_0\right)_{BA} (\mathbb{1}+\gamma_0)_{AC}\Gamma^0_{CD}\; q^b_D(\mathbf{x},0)\; \bar{q}^a_B(\mathbf{x},t) \\
\xrightarrow{\mathcal{P}^{tm}} &\left(\gamma_0\Gamma^{t,\dagger}\gamma_0\right)_{BA} (\mathbb{1}+\gamma_0)_{AC}\Gamma^0_{CD}\; (\gamma_0)_{DS} q^b_S(\mathbf{x},0)\; \bar{q}^a_T(-\mathbf{x},t)(\gamma_0)_{TB} \\
= &\; (\gamma_0)_{TB}\left(\gamma_0\Gamma^{t,\dagger}\gamma_0\right)_{BA} (\mathbb{1}+\gamma_0)_{AC}\Gamma^0_{CD}\; (\gamma_0)_{DS} q^b_S(\mathbf{x},0)\; \bar{q}^a_T(-\mathbf{x},t) \\
= &\left(\gamma_0\gamma_0\Gamma^{t,\dagger}\gamma_0(\mathbb{1}+\gamma_0)\Gamma^0\;\gamma_0\right)_{TS} q^b_S(\mathbf{x},0)\; \bar{q}^a_T(-\mathbf{x},t)
\end{aligned} \tag{3.8}$$

It follows, that

- Contractions with exchanged flavours have to be related, i.e. $u \leftrightarrow d$,
- $\Gamma \leftrightarrow \gamma_0\Gamma\gamma_0$, i.e. sign change for $\Gamma \in \{\gamma_5, \gamma_0\gamma_5\}$.

Charge conjugation $\mathcal{C}$

$$\begin{aligned}
&\left(\gamma_0\Gamma^{t,\dagger}\gamma_0\right)_{BA} (\mathbb{1}+\gamma_0)_{AC}\Gamma^0_{CD}\; q^b_D(0)\; \bar{q}^a_B(t) \\
\xrightarrow{\mathcal{C}} &\left(\gamma_0\Gamma^{t,\dagger}\gamma_0\right)_{BA} (\mathbb{1}+\gamma_0)_{AC}\Gamma^0_{CD}\; (\gamma_0\gamma_2)_{DS} \bar{q}^{b,T}_S(0)\; (-1) q^{a,T}_T(t)(\gamma_2\gamma_0)_{TB} \\
= &\; (\gamma_2\gamma_0)_{TB}\left(\gamma_0\Gamma^{t,\dagger}\gamma_0\right)_{BA} (\mathbb{1}+\gamma_0)_{AC}\Gamma^0_{CD}\; (\gamma_0\gamma_2)_{DS} \bar{q}^{b,T}_S(0)\; (-1) q^{a,T}_T(t) \\
= &\left(\gamma_2\gamma_0\gamma_0\Gamma^{t,\dagger}\gamma_0(\mathbb{1}+\gamma_0)\Gamma^0\;\gamma_0\gamma_2\right)_{TS} \bar{q}^{b,T}_S(0)\; (-1) q^{a,T}_T(t) \\
= &\left(\gamma_2\gamma_0\gamma_0\Gamma^{t,\dagger}\gamma_0(\mathbb{1}+\gamma_0)\Gamma^0\;\gamma_0\gamma_2\right)_{ST} q^a_T(t)\; \bar{q}^b_S(0) \\
\overset{t\to -t}{=} &\left(\gamma_2\gamma_0\gamma_0\Gamma^{t,\dagger}\gamma_0(\mathbb{1}+\gamma_0)\Gamma^0\;\gamma_0\gamma_2\right)_{ST} q^a_T(0)\; \bar{q}^b_S(-t)
\end{aligned} \tag{3.9}$$

The symmetry transformation rules are:

- Contractions computed in positive and negative time direction have to be related, i.e. $+t \leftrightarrow -t$.
- $\Gamma \leftrightarrow \gamma_2\gamma_0\Gamma^T\gamma_0\gamma_2$, i.e. sign change for $\Gamma \in \{\gamma_0\}$.

Once the contractions have been computed, all the above listed rules will be applied to every single contraction, i.e. the arithmetic mean of contractions related by those symmetries is computed. Since related contractions only differ within computational fluctuations, this procedure gives rise to an improvement of statistical errors. Moreover, they allow for a verification of the computed contractions with respect to these symmetries, i.e. if they have large differences in their value or even in their shapes the computed contractions might be corrupt.

3.3 General eigenvalue problem

The general eigenvalue problem is one way to extract the desired effective hadron masses [2], [12]. The idea is to combine different operators $\mathcal{O}_0, \mathcal{O}_1, \ldots$ with respect to

the states we want to investigate to a correlation matrix $C(t)$

$$\begin{aligned} C_{ij}(t) &= \langle\Omega|\, \mathcal{O}_i(t)^\dagger \mathcal{O}_j(0)\, |\Omega\rangle \\ &= \sum_n \langle\Omega|\, \mathcal{O}_i^\dagger\, |n\rangle \langle n|\, \mathcal{O}_j\, |\Omega\rangle\, e^{-E_n t}. \end{aligned} \tag{3.10}$$

Since we investigate two different states collected in a 2×2-correlation matrix, we have to solve the two dimensional general eigenvalue problem

$$C(t)\, \mathbf{u}^{(k)}(t, t_r) = \lambda^{(k)}(t, t_r)\, C(t_r)\, \mathbf{u}^{(k)}(t, t_r) \tag{3.11}$$

where $\lambda^{(k)}$ are the eigenvalues and $\mathbf{u}^{(k)}$ the corresponding eigenvectors belonging to the k-th state. The reference time t_r leads to a reduction of contributions from higher states which in turn improves the signal for contributions of lower states. The eigenvalues are then proportional to the desired exponentials

$$\lambda^{(k)}(t, t_r) \propto e^{-E_k(t-t_r)} \left(1 + \mathcal{O}\left(e^{-\Delta E_k(t-t_r)}\right)\right), \tag{3.12}$$

where E_k is the energy value of the k-th state and ΔE_k the difference with regard to the lowest lying energy state, respectively.

This method is applied to the correlation matrix $C(t)$ for every time step t. Since it is possible that the calculated eigenvalues of different states take similar values, it might be difficult to assign these to the corresponding states. In those cases the eigenvector components $\mathbf{u}_j^{(k)}$ have to be taken into consideration which give information about the contribution of the k-th state to the j-th operator of the correlation matrix.

The effective masses are then calculated as in the case of single state correlators described in section 2.2:

$$a\, m_{\text{eff}}^{(k)}(t) = \ln\left(\frac{\lambda^{(k)}(t, t_r)}{\lambda^{(k)}(t + a, t_r)}\right) \tag{3.13}$$

These effective masses are then fitted in a suitable range $t_{min}, \ldots, t_{max}$, i.e. which reduces the errors at most.

3.4 Techniques for propagator computation

On the lattice, sources provide the possibility to calculate parts of the fermion propagator D^{-1}. The Dirac matrix D has $\mathcal{O}(10^{12})$ elements and although they're sparsely distributed, D^{-1} will also have as many elements which are not necessarily sparse. Due to the lack of memory to store such an amount of data and for numerical cost reasons, only columns of the propagator are calculated [2].

We have to solve the following equations:

$$\sum_y D^{(f)}_{a,A;b,B}(x,y)G^{(f)}_{b,B;c,C}(y,z) = \delta_{a,c}\delta_{A,C}\delta(x,z) \tag{3.14}$$

Due to the high amount of equations we have to solve $(12 \times T \times L^3)$, we only compute estimations for the full propagator which will be discussed in the following sections.

3.4.1 Point-to-all propagators

These propagators make use of translational invariance and hence are computed from a single spacetime point x to every other spacetime point y. To get one column of the quark propagator, one has to obtain a solution for a combination of colour and spin indices, i.e. $3 \times 4 = 12$ solutions of a linear system of the form

$$\sum_y D^{(f)}_{a,A;b,B}(x,y)\phi^{(f)}_{b,B}(y)[c,C,z] = \xi_{a,A}(x)[c,C,z], \quad \xi_{a,A}(x)[c,C,z] = \delta_{a,c}\delta_{A,C}\delta(x,z). \tag{3.15}$$

The indices c and C label 12 different point sources $\xi_{a,A}(x)[c,C,z]$ for a fixed spacetime point z, whereas each solution $\phi^{(f)}_{b,B}(y)[c,C,z]$ represents a single column of the inverse Dirac matrix D. The sought point-to-all propagator reads

$$\phi^{(f)}_{b,B}(y)[a,A,x] = G^{(f)}_{b,B;a,A(x,y)} \tag{3.16}$$

3.4.2 Stochastic timeslice-to-all propagators

Due to the problem, that the exact computation of the point-to-all propagator is not possible in practice, the propagator is usually estimated by statistical methods. A commonly used approach is the so called stochastic timeslice-to-all propagator. In contrast to the mentioned point-to-all propagators, in this case the propagator is computed from any spatial point in a given timeslice to any other spacetime point. The linear systems remain the same except the source term and its labelling changes to $n \in 1, ..., N$:

$$\sum_y D^{(f)}_{a,A;b,B}(x,y)\phi^{(f)}_{b,B}(y)[t_0,n] = \xi_{a,A}(x)[t_0,n], \quad \xi_{a,A}(x)[t_0,n] = \delta_{x_0,t_0}\Xi_{a,A}(\mathbf{x})[n], \tag{3.17}$$

where $\Xi_{a,A}(\mathbf{x})[n]$ are uniformly distributed random numbers fulfilling

$$\frac{1}{N}\sum_{n=1}^{N} \Xi_{a,A}(\mathbf{x})[n]^*\Xi_{b,B}(\mathbf{y})[n] = \delta_{a,b}\delta_{A,B}\delta(\mathbf{x},\mathbf{y}) + \text{unbiased noise}. \tag{3.18}$$

A common choice is $\Xi_{a,A}(\mathbf{x})[n] \in \mathbb{Z}_2 \times \mathbb{Z}_2$ which results in an unbiased noise proportional to $\mathcal{O}(1/\sqrt{N})$.

This results in the propagator

$$G^{(f)}(y;\mathbf{x},t_0) = \frac{1}{N}\sum_{n=1}^{N}\phi^{(f)}(y)[t_0,n](\xi(\mathbf{x},t_0)[t_0,n])^\dagger + \text{unbiased noise}, \tag{3.19}$$

which will be mostly used for our lattice computations which always include light quark fields.

3.4.3 One-end trick

The one-end trick is a way to compute a product of two propagators but is only possible for products of the form

$$\sum_{\mathbf{y}} G^{(f_1)}(x;\mathbf{y},t)\,\Gamma\,G^{(f_2)}(\mathbf{y},t;z), \tag{3.20}$$

i.e. the propagators are connected at every spacetime point $(\mathbf{y},t)$, but no further propagators start or end at $(\mathbf{y},t)$ which fits a meson correlator. The linear systems then have the form

$$D^{(f_1)}_{a,A;b,B}(x;y)\,\phi^{(f_1)}_{b,B}(x)[t_0,n] = \xi_{a,A}(y)[t_0,n] \tag{3.21}$$

$$D^{(f_2)}_{a,A;b,B}(x;y)\,\tilde{\phi}^{(f_2)}_{b,B}(x)[t_0,\Gamma,n] = (\gamma_5\,\Gamma^\dagger\,\xi)_{a,A}(y)[t_0,n], \tag{3.22}$$

where ξ are stochastic timeslice sources as defined in (3.17). ϕ and $\tilde{\phi}$ then express the propagators' product (3.20) as

$$\sum_{\mathbf{y}} G^{(f_1)}(x;\mathbf{y},t)\,\Gamma\,G^{(f_2)}(\mathbf{y},t;z) = \frac{1}{N}\sum_{n=1}^{N}\phi^{(f_1)}(x)[t,n]\,\tilde{\phi}^{(f_2)}(z)[t,\Gamma,n]^\dagger\gamma_5 + \text{unbiased noise} \tag{3.23}$$

3.5 tmLQCD Software Suite - Inverter

The tmLQCD Software Suite, see [13], is a collection of programmes for the simulation of (twisted mass) Qunatum Chromodynamics on a four dimensional spacetime lattice. Despite of the potential for generating gauge configurations with the help of the Hybrid Monte Carlo Algorithm, see [14], which is implemented in the binary `hmc_tm`, this programme suite also provides an implementation for the computation of quark propagators in the binary `invert`. In addition to gauge configurations these propagators are needed for many lattice computations including light quarks in their observables such as those we are interested in.

Usually, the gauge configurations used are directly obtained from the European Twisted Mass Collaboration (ETMC) from which the quark propagators are computed to our needs, i.e. the explicit sources are computed by us in accordance to section 3.4. Even though the programme `gen_sources` is capable of computing various source types by

itself, stochastic timeslice sources are not provided yet. Therefore, we can rely on an own implementation of (3.17) as well as the high quality random number generator *RANLUX* introduced by M.Lüscher, see [15].

The input for the `invert` programme then consists of two files: The source generated as mentioned above and a file with a list of parameters describing the lattice proportions and characteristics as well as the physical parameters like the quark mass.

In fact, the `invert` programme uses the discretised version of the twisted mass action (2.4), [3]:

$$S_{light} = a^4 \sum_x \bar{\chi}(x) \left(D_W + m_0 + i\mu\gamma_5\sigma_3 \right) \chi(x) \tag{3.24}$$

where χ denotes the light quark field in the twisted basis which is related to the physical basis via the twist rotation (2.5). D_W denotes the Wilson-Dirac operator

$$D_W = \frac{1}{2} \left(\gamma_\mu \left(\nabla_\mu + \nabla^*_\mu \right) - a \nabla^*_\mu \nabla_\mu \right), \tag{3.25}$$

μ is referred to as the twisted mass parameter and σ_3 is the third Pauli matrix. ∇_μ and ∇^*_μ are the standard gauge covariant forward and backward derivatives. In the end, the desired propagators are computed by inverting the Dirac matrix.

3.6 BB systems

3.6.1 Gauge transformation test

In order to verify the correctness of the implemented correlator in the code one can choose from several methods. One of the most powerful method is a gauge invariance test. Since the whole theory is constructed to be locally gauge invariant, the observables we are interested in have to be constructed in a gauge invariant manner, too, i.e. they are asymptotic colour singlets. A simple way of implementing such a test is to apply a random gauge transformation $g(n) \in SU(3)$ on the field variables $\psi(n)$ at each lattice site $n \in \{0, \ldots, L-1\}^3 \times \{0, \ldots, T-1\}$ as well as on every link variable $U(n, n+\hat{\mu})$. Here, $g(n)$ depends on n because gauge symmetry is a local symmetry with the following well known transformation rules

$$\begin{aligned} U(n+\hat{\mu}) &\to U'(n+\hat{\mu}) = g(n) U(n+\hat{\mu}) g(n+\hat{\mu})^\dagger, \\ \psi(n) &\to \psi'(n) = g(n)\psi(n), \\ \bar{\psi}(n) &\to \bar{\psi}'(n) = \bar{\psi}(n) g(n)^\dagger. \end{aligned} \tag{3.26}$$

A comparison of the computed observables once with and once without a random gauge transformation should give the same results within computational errors. Visually this is comparable to unconnected pieces in the system's diagram, see e.g. 2.3. A gauge invariant observable always has no disconnected pieces in its diagram because

these would imply that there are different, non matching local gauge transformations $g(n), g(m),\ n \neq m$ rendering the observable gauge invariant. Therefore, this approach suits best to detect mistakes made in the geometry of an implemented observable. In combination with the elimination of degrees of freedom those mistakes can be located in subsequent step.

Since the quark fields are implemented by the sources and sinks introduced in section 3.4, we have to apply the gauge transformation within our calculation on those, respectively [16]:

$$\begin{aligned} U(x,y) &\to g(x)U(x,y)g(y)^\dagger \\ \phi(x) &\to g(x)\phi(x) \\ \xi(x) &\to g(x)\xi(x) \end{aligned}$$

A possible strategy to implement a random gauge transformation is to generate $L^3 \times T$ matrices $A(n)$ with uniformly distributed entries $A(n)_{ij} \sim \text{unif}(-1, 1)$ which will be projected onto a matrix $g(n) \in SU(3)$. Subsequently, these are multiplied with the gauge field and spinor field, respectively.

3.7 BB correlator

In principle, the implementation of BB systems follows that of the B mesons. The algorithm can be described as follows: Here, we have to keep in mind that the separa-

for *all spatial separations,*
all temporal separations
and all z' **do**
Connect the static quarks at x and y with the corresponding links $U(x,0;z,0)$ and $U(z,0;y,0)$ to the space time point $(z,0)$.
Connect the static quarks in temporal direction with $U(x,0;x,t)$ and $U(y,0;y,t)$.
Close the loop with gauge links $U(x,t;z',t)$ and $U(z',t;y,t)$.
end

Algorithm 1: Strategy to compute the BB correlator

tion r can take even and odd values, i.e. z and z' respectively have different distances in lattice units to the static quarks. This can be taken into account by implementing a geometry of choice, for example choosing one gauge link to take odd values. The first helpful step towards the implementation of the BB correlation function is test the geometry independently which results in static quark potentials.

Due to the fact that BB mesons are essentially two B mesons, one can test the implementation by computing the "half" BB correlator including its geometry and light

quark propagator. This has the advantage that the Levi-Civita or the Kroencker delta smybols respectively can be excluded from the equation leading to less complex implementations of the correlator. Furthermore, choosing meaningful parameters, especially setting one of the extensions T and L to zero to eliminate sources for mistakes, ist quite helpful.

Combined with the gauge transformation test described in section 3.6.1, this is a powerful framework to detect and locate misleading implementations on the way to a well working correlator giving the desired results.

Chapter 4

Numerical results

In this chapter we will present the numerical results. The computations were performed with three ensembles of gauge configurations with $N_f = 2$ dynamical quark flavours which were generated by the ETCM. As described in section 2.3, these configurations were generated for the maximal twist for the $\mathcal{O}(a)$ improvement of discretization errors. Furthermore, the gauge configurations differ in the bare quark masses, i.e. we used those with $\mu = 0.015, 0.085, 0.004$ as shown in 3.1. The light quark propagators are addressed with 12 timeslice sources, see section 3.4, per flavour and configuration. Moreover, the observable's maximal temporal separation was 18.

The signal quality of the correlation functions computed, was improved by utilizing APE smearing for the spatial links with parameters $N_{\mathrm{APE}} = 10$, $\alpha_{\mathrm{APE}} = 0.5$, Gaussian smearing with parameters $N_{\mathrm{Gauss}} = 30$, $\kappa_{\mathrm{Gauss}} = 0.5$ as well as HYP smearing with parameters $N_{\mathrm{HYP}} = 1$, $\alpha_{\mathrm{HYP}} = (1.0, 1.0, 0.5)$.

4.1 Correlators

The first numerical results we want to present are the computed correlators $C_{ij},\ i, j \in \{0, 1\}$. They are subject to statistical error improvements, see section 3.2, as well as the basic building blocks for the computation of effective masses, see for single-state correlations section 2.2 and for multi-state correlations section 3.3. Moreover, a first indicator for the effective mass is directly visible through the exponential decay of the curve predicted by our theory. This can be considered a first check for the integrity of the lattice calculation but we have to keep in mind that, with respect to certain symmetries, also other shapes occur. These two contractions are very similar because both are calculated in the same channel $\gamma_1 - \gamma_5$. As explained in section 3.2, these and all other by a symmetry related contractions are combined and their average values are calculated to reduce statistical errors. A visible comparison is shown in figure 4.2.

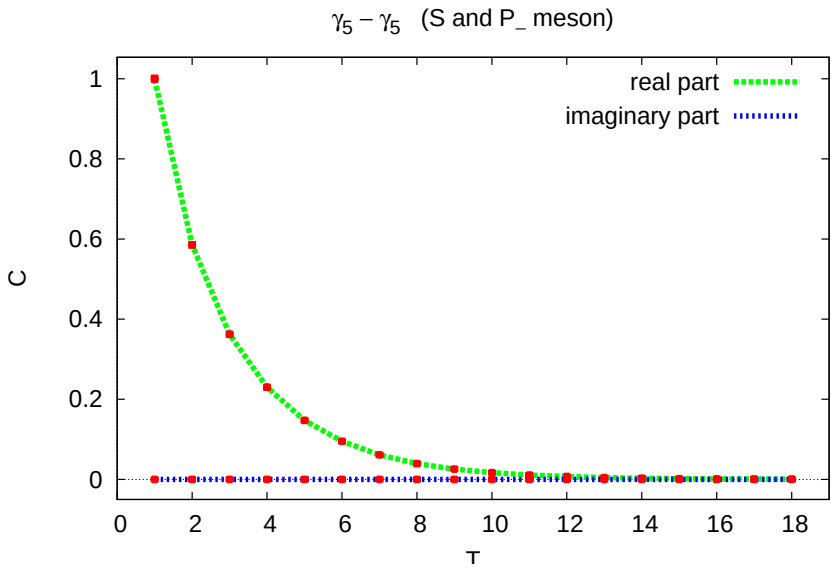

FIGURE 4.1: Contraction with a bare quark mass of $\mu = 0.015$ in lattice units illustrated for the γ_5-γ_5 correlator.

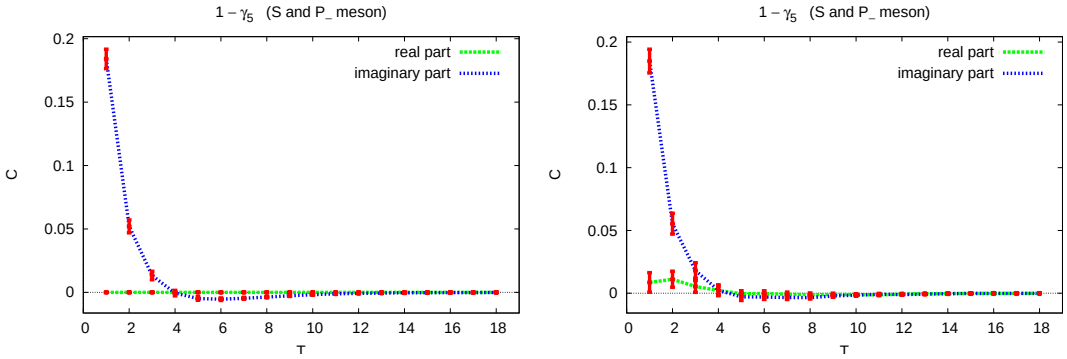

(a) (b)

FIGURE 4.2: Comparison of the symmetry averaging for (a) correlator before symmetry averaging and (b) correlator after symmetry averaging both for $\mu = 0.15$.

4.2 Static light meson masses

This section shows the numerical results of the computation of the static light meson masses we are interested in. As described in section 3.3, one possibility to extract these effective masses is to build the correlation matrix C and to solve the general eigenvalue problem regarding C.

In figure 4.3 a plot of the effective mass m_{eff} as a function of the time T in lattice units is shown. Moreover, for both states, the occurring plateau is fitted with a linear ansatz. Note that these fits only include a specific range of points in time $T \in \{t_{min}, \ldots, t_{max}\}$ in accordance to obtain physically reasonable results. First of all, points in time before the computed effective mass reaches a plateau have to be discarded. Moreover, the errors shown in figure 4.3 increase heavily with increasing

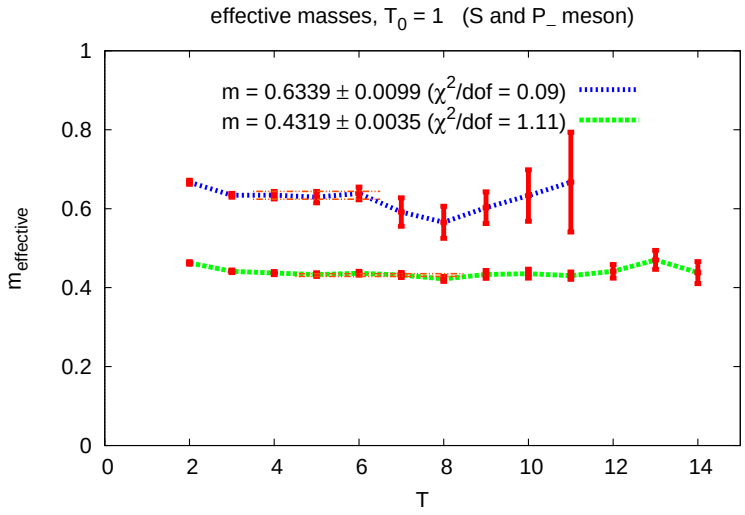

FIGURE 4.3: Effective masses for the bare quark mass $\mu = 0.015$ in lattice units

T due to the decreasing signal to noise ratio caused by the exponential decay of the signal while the errors remain constant over all points in time. This leads to large statistical errors, i.e. points in time beyond a certain value for T have to be discarded as well. However, the signal to noise ratio can be improved by increasing the amount of configurations used. In terms of finding a suitable t_{max}, a possible strategy is to fit the plateau for various values of t_{min} and t_{max} and look for those which minimise the value for the reduced χ^2 value. The values for the S and the P_- state for three different quark masses are shown in table 4.1.

$j^{\mathcal{P}}$	$\mu = 0.004$	$\mu = 0.0085$	$\mu = 0.015$
$(1/2)^- \equiv S$	3.30	1.17	1.11
$(1/2)^+ \equiv P$	0.23	1.15	0.09

TABLE 4.1: Reduced χ^2/dof value for the S and P_- state for different bare quark masses μ

While for $\mu = 0.085$ both states and for $\mu = 0.015$ the S state show decently reasonable reduced χ^2 values, the other values are exceptionally different from 1, see also figure 4.5b. If we compare these cases with the effective mass plots in figure 4.3 and figure 4.5, the decent values match the observation of larger fitting ranges.

In figure 4.4 the eigenvector components computed from the correlation matrix C with the general eigenvalue problem are shown. In the computation of the correlation

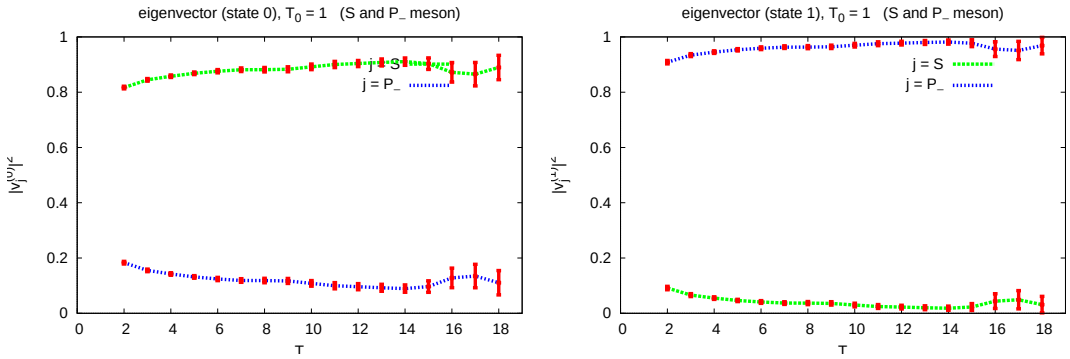

(a) (b)

FIGURE 4.4: Eigenvector components $|v_j^{(k)}|^2$ for a bare quark mass of $\mu = 0.015$ for (a) the ground state and for (b) the first excited state

matrix every operator used represents one of the states we are interested in. The eigenvector components describe the shares of each operator used in the computation of the correlation function in the respective state we took as the basis for this calculation. On the left the eigenvector components of the ground state and on the right the eigenvector components of the first excited state are presented, respectively. The expectation we have, is that the states S and P_- spread perfectly over the first and second state. This means that the components of the first state should be 1 for all points in time for the operator representing the S state and 0 for all points in time representing the P_- state. The fact that the eigenvector components are not perfectly shared amongst the given operators has its reason in statistical fluctuations.
Nevertheless, this allows us to assign the results for the effective masses to the corresponding states. This can be quite difficult if the values of the effective masses are close together and hence are not differentiable. In this case the S state has an effective mass of $\hat{m}_{\text{eff}}(S) = 0.4319$ in lattice units while the P_- state has an effective mass of $\hat{m}_{\text{eff}}(P_-) = 0.6339$ in lattice units.

4.3 Chiral limit

One problem of lattice computations for QCD are the unphysically high quark masses which can be tuned by the bare quark mass μ. There are two important numerical reasons that it is hardly achievable to perform lattice computations with physical quark masses. First, the finite size effects increase in such a manner that the amount of lattice sites has to increase vastly [2]. Furthermore, the eigenvalues of the Dirac matrix become smaller for physical quark masses and hence the numerical costs for inversions of the Dirac matrix to obtain light quark propagators increase [1]. As progress over the past decades in terms of computer power as well as numerical methods was made, the expectation follows the trend for a approach towards physical quark masses

However, common practice is to compute the effective masses for different bare quark masses μ and lattice spacings a and to extrapolate the results to the physical quark mass. This is called the chiral limit. In this scope, we will only make use of the variation of the bare quark mass. In addition to the discussed effective mass computed with the bare quark mass $\mu = 0.015$ in section 4.2, figure 4.5 shows the effective masses for the other ensembles we used for the computation. Moreover, the effective masses are collected in table 4.2 in lattice units.

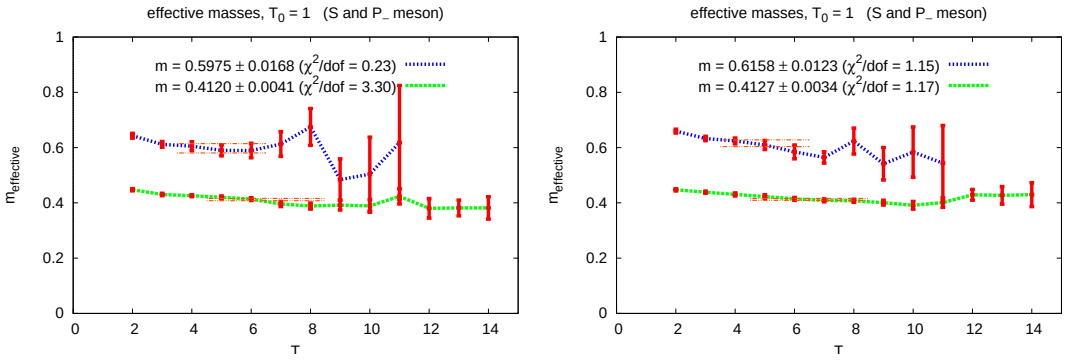

(a) (b)

FIGURE 4.5: Effective masses in lattice units for bare quark masses of (a) $\mu = 0.040$ and (b) $\mu = 0.085$.

$j^{\mathcal{P}}$	$\mu = 0.004$	$\mu = 0.0085$	$\mu = 0.015$
$(1/2)^- \equiv S$	0.4120	0.4127	0.4319
$(1/2)^+ \equiv P_-$	0.5975	0.6158	0.6339

TABLE 4.2: Effective masses $\hat{m}_{\text{eff}}$ computed with different quark masses in lattice units

To obtain the physical effective masses, the S state is utilized as reference level, i.e. we calculate the difference $m_{\text{eff}}(P_-) - m_{\text{eff}}(S)$ for the three different bare quark masses. This is necessary because the static quarks in the the B meson are located sharply due to their infinite mass. In the continuum this leads to an infinite self-energy while on the lattice the self-energy is finite within the locational boundary of the lattice spacing a, i.e. decreasing the lattice spacing increases the self-energy and vice versa. By means of the lattice spacing $a = 0.0855fm$, see table 3.1, we end up with

$$m_{\text{eff}}(P_-) - m_{\text{eff}}(S) = \frac{\hat{m}_{\text{eff}}(P_-) - \hat{m}_{\text{eff}}(S)}{a}, \tag{4.1}$$

resulting in the effective masses of the P_- state in MeV collected in table 4.3.

$j^{\mathcal{P}}$	$\mu = 0.004$	$\mu = 0.0085$	$\mu = 0.015$
$(1/2)^+ \equiv P_-$	428(29)	468(20)	466(15)

TABLE 4.3: Effective masses m_{eff} computed with different quark masses in MeV

To obtain the effective mass at as physical u/d quark mass, the effective masses for the different bare quark masses are subject to a regression. Due to the linear behaviour of effective masses as a function of the squared mass m_{PS}^2, it is most convenient to utilize this for a linear regression which also benefits the visual expression, see figure 4.6 where the effective mass differences for the P_- state are plotted as a function of m_{PS}^2 including a green straight line as a result of the linear regression which is suitable within the scope of errors resulting from the lattice computation and a vertical black line marking the physical u/d quark mass.

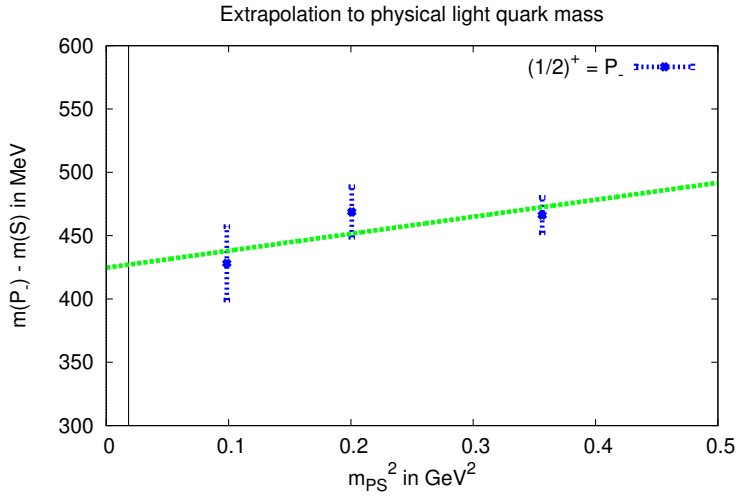

FIGURE 4.6: Extrapolation to physical u/d quark mass. The effective mass of the P_- state with regard to the effective mass of the S state is shown. The vertical black line indicates the physical u/d quark mass.

The extrapolation results in an effective mass difference of $m_{\text{eff}}(P_-) - m_{\text{eff}}(S) = 427(24)$ MeV at physical u/d quark mass. This result alongside the results for the effective masses obtained for the different bare quark masses match and verify the results in [17] to a great extent.

Chapter 5

Conclusions

5.1 Summary

In this thesis we gave and introduction to the framework of twisted mass lattice QCD as a equivalent formulation of standard continuum theory with an improvement in finite size effects for computed observables. We gave an overview of the concepts of twisted mass lattice QCD with regard to the computation of hadron spectroscopy in terms of B mesons and their effective masses. We described those mesons by their quantum numbers and symmetries as well as their trial states and correlators.

We computed the effective masses of B mesons by means of gauge configurations generated with $N_f = 2$ dynamical quark flavours for different bare quark masses μ and extrapolated the effective masses obtained in m_{PS}^2 to the physical u/d quark mass.
In addition we gave a broad overview of the techniques used in lattice QCD computations to not only allow for meaningful results but also for statistical improvements. These were introduced for B mesons as well as BB mesons.

Furthermore, we introduced the concept of four-quark systems within the scope of different tetraquark structures, i.e. the mesonic molecule and the diquark-antidiquark state which allow for a better understanding of bound four-quark states addressing the recent progression in detecting those in experiments.

5.2 Outlook

In the end we want to give a short outlook for further investigations regarding B and BB mesons. For the former it is desirable to compute effective masses for more than the bare quark masses we used and also to account for different lattice spacings a. It is imaginable that with more powerful hardware the physical u/d quark mass will be within range in the upcoming future as it has been approached over the past decades. For BB systems it is desirable to compute potentials from an actual implementation

of the correlator of diquark-antidiquark states and compare the results with those of the mesonic molecule to obtain more insight into the area of particle physics.

Appendix A

A.1 Relation between twisted basis and physical basis

A.1.1 Twisted basis

Case 1: $\Gamma_t = \gamma_5, \Gamma_0 = \gamma_5$

$$\begin{aligned}\Gamma &= \gamma_0\Gamma_t^\dagger\gamma_0(\mathbb{1}+\gamma_0)\Gamma_0 \\ &= -\gamma_5(\mathbb{1}+\gamma_0)\gamma_5 \\ &= -(\mathbb{1}+\gamma_5\gamma_0\gamma_5) \\ &= -(\mathbb{1}-\gamma_0) \\ &= \gamma_0 - 1 \end{aligned} \tag{A.1}$$

Case 2: $\Gamma_t = \gamma_5, \Gamma_0 = \mathbb{1}$

$$\begin{aligned}\Gamma &= \gamma_0\Gamma_t^\dagger\gamma_0(\mathbb{1}+\gamma_0)\Gamma_0 \\ &= -\gamma_5(\mathbb{1}+\gamma_0)\mathbb{1} \\ &= -(\gamma_5+\gamma_5\gamma_0) \\ &= -(\gamma_5-\gamma_0\gamma_5) \\ &= \gamma_0\gamma_5 - \gamma_5 \end{aligned} \tag{A.2}$$

Case 3: $\Gamma_t = \mathbb{1}, \Gamma_0 = \gamma_5$

$$\begin{aligned}&= \gamma_0\Gamma_t^\dagger\gamma_0(\mathbb{1}+\gamma_0)\Gamma_0 \\ &= \mathbb{1}(\mathbb{1}+\gamma_0)\gamma_5 \\ &= \gamma_5 + \gamma_0\gamma_5 \end{aligned} \tag{A.3}$$

Case 4: $\Gamma_t = \mathbb{1}, \Gamma_0 = \mathbb{1}$

$$\begin{aligned}&= \gamma_0\Gamma_t^\dagger\gamma_0(\mathbb{1}+\gamma_0)\Gamma_0 \\ &= \mathbb{1}(\mathbb{1}+\gamma_0)\mathbb{1} \\ &= \mathbb{1} + \gamma_0 \end{aligned} \tag{A.4}$$

A.1.2 Physical basis

Case 1, $\Gamma_t = \gamma_5, \Gamma_0 = \gamma_5$

$$\begin{aligned}
C_{55}^{pb} &= \left(\mathcal{O}_5^{pb}\right)^\dagger \mathcal{O}_5^{pb} \\
&= \frac{1}{\sqrt{2}}\left(\left(\mathcal{O}_5^{tb}\right)^\dagger \mp i\left(\mathcal{O}_1^{tb}\right)^\dagger\right)\frac{1}{\sqrt{2}}\left(\mathcal{O}_5^{tb} \pm i\mathcal{O}_1^{tb}\right) \\
&= \frac{1}{2}\left(\left(\mathcal{O}_5^{tb}\right)^\dagger \mathcal{O}_5^{tb} \mp i\left(\mathcal{O}_1^{tb}\right)^\dagger \mathcal{O}_5^{tb} \pm i\left(\mathcal{O}_5^{tb}\right)^\dagger \mathcal{O}_1^{tb} + \left(\mathcal{O}_1^{tb}\right)^\dagger \mathcal{O}_1^{tb}\right) \\
&= \frac{1}{2}\left(C_{55}^{tb} \mp iC_{15}^{tb} \pm iC_{51}^{tb} + C_{11}^{tb}\right) \\
&\widehat{=} \frac{1}{2}\left(\gamma_0 - \mathbb{1} \mp i(\gamma_0\gamma_5 + \gamma_5 - (\gamma_0\gamma_5 - \gamma_5)) + \gamma_0 + \mathbb{1}\right) \\
&= \gamma_0 \mp i\gamma_5
\end{aligned} \tag{A.5}$$

Case 2, $\Gamma_t = \gamma_5, \Gamma_0 = \mathbb{1}$

$$\begin{aligned}
C_{51}^{pb} &= \left(\mathcal{O}_5^{pb}\right)^\dagger \mathcal{O}_1^{pb} \\
&= \frac{1}{\sqrt{2}}\left(\left(\mathcal{O}_5^{tb}\right)^\dagger \mp i\left(\mathcal{O}_1^{tb}\right)^\dagger\right)\frac{1}{\sqrt{2}}\left(\mathcal{O}_1^{tb} \pm i\mathcal{O}_5^{tb}\right) \\
&= \frac{1}{2}\left(\left(\mathcal{O}_5^{tb}\right)^\dagger \mathcal{O}_1^{tb} \mp i\left(\mathcal{O}_1^{tb}\right)^\dagger \mathcal{O}_1^{tb} \pm i\left(\mathcal{O}_5^{tb}\right)^\dagger \mathcal{O}_5^{tb} + \left(\mathcal{O}_1^{tb}\right)^\dagger \mathcal{O}_5^{tb}\right) \\
&= \frac{1}{2}\left(C_{51}^{tb} \mp iC_{11}^{tb} \pm iC_{55}^{tb} + C_{15}^{tb}\right) \\
&\widehat{=} \frac{1}{2}\left(\gamma_0\gamma_5 - \gamma_5 \mp i(\gamma_0 + \mathbb{1} - (\gamma_0 - \mathbb{1})) + \gamma_0\gamma_5 + \gamma_5\right) \\
&= \gamma_0\gamma_5 \mp i\mathbb{1}
\end{aligned} \tag{A.6}$$

Case 3, $\Gamma_t = \mathbb{1}, \Gamma_0 = \gamma_5$

$$\begin{aligned}
C_{15}^{pb} &= \left(\mathcal{O}_1^{pb}\right)^\dagger \mathcal{O}_5^{pb} \\
&= \frac{1}{\sqrt{2}}\left(\left(\mathcal{O}_1^{tb}\right)^\dagger \mp i\left(\mathcal{O}_5^{tb}\right)^\dagger\right)\frac{1}{\sqrt{2}}\left(\mathcal{O}_5^{tb} \pm i\mathcal{O}_1^{tb}\right) \\
&= \frac{1}{2}\left(\left(\mathcal{O}_1^{tb}\right)^\dagger \mathcal{O}_5^{tb} \mp i\left(\mathcal{O}_5^{tb}\right)^\dagger \mathcal{O}_5^{tb} \pm i\left(\mathcal{O}_1^{tb}\right)^\dagger \mathcal{O}_1^{tb} + \left(\mathcal{O}_5^{tb}\right)^\dagger \mathcal{O}_1^{tb}\right) \\
&= \frac{1}{2}\left(C_{15}^{tb} \mp iC_{55}^{tb} \pm iC_{11}^{tb} + C_{51}^{tb}\right) \\
&\widehat{=} \frac{1}{2}\left(\gamma_0\gamma_5 + \gamma_5 \mp i(\gamma_0 - \mathbb{1} - (\gamma_0 + \mathbb{1})) + \gamma_0\gamma_5 - \gamma_5\right) \\
&= \gamma_0\gamma_5 \pm i\mathbb{1}
\end{aligned} \tag{A.7}$$

Case 4, $\Gamma_t = \mathbb{1}, \Gamma_0 = \mathbb{1}$

$$\begin{aligned}
C_{11}^{pb} &= \left(\mathcal{O}_1^{pb}\right)^\dagger \mathcal{O}_1^{pb} \\
&= \frac{1}{\sqrt{2}}\left(\left(\mathcal{O}_1^{tb}\right)^\dagger \mp i\left(\mathcal{O}_5^{tb}\right)^\dagger\right)\frac{1}{\sqrt{2}}\left(\mathcal{O}_1^{tb} \pm i\mathcal{O}_5^{tb}\right) \\
&= \frac{1}{2}\left(\left(\mathcal{O}_1^{tb}\right)^\dagger \mathcal{O}_1^{tb} \mp i\left(\mathcal{O}_5^{tb}\right)^\dagger \mathcal{O}_1^{tb} \pm i\left(\mathcal{O}_1^{tb}\right)^\dagger \mathcal{O}_5^{tb} + \left(\mathcal{O}_5^{tb}\right)^\dagger \mathcal{O}_5^{tb}\right) \\
&= \frac{1}{2}\left(C_{11}^{tb} \mp iC_{51}^{tb} \pm iC_{15}^{tb} + C_{55}^{tb}\right) \\
&\widehat{=} \frac{1}{2}\left(\gamma_0 + \mathbb{1} \mp i(\gamma_0\gamma_5 - \gamma_5 - (\gamma_0\gamma_5 + \gamma_5)) + \gamma_0 - \mathbb{1}\right) \\
&= \gamma_0 \pm i\gamma_5
\end{aligned} \tag{A.8}$$

A.1.3 Summary

Gammas	Twisted basis	Physical basis
$\Gamma_t = \gamma_5, \Gamma_0 = \gamma_5$	$\gamma_0 - \mathbb{1}$	$\gamma_0 - i\gamma_5$
$\Gamma_t = \gamma_5, \Gamma_0 = \mathbb{1}$	$\gamma_0\gamma_5 - \gamma_5$	$\gamma_0\gamma_5 - i$
$\Gamma_t = \mathbb{1}, \Gamma_0 = \gamma_5$	$\gamma_0\gamma_5 + \gamma_5$	$\gamma_0\gamma_5 + i$
$\Gamma_t = \mathbb{1}, \Gamma_0 = \mathbb{1}$	$\gamma_0 + \mathbb{1}$	$\gamma_0 + i\gamma_5$

A.2 Correlators

A.2.1 B meson correlator in matrix vector notation

$$\begin{aligned}
C &= \langle\Omega|\, \mathcal{O}^\dagger(t)\mathcal{O}(0)\,|\Omega\rangle \\
&= \langle\Omega|\, \left(\bar{Q}(t)\Gamma_t\psi(t)\right)^\dagger \bar{Q}(0)\Gamma_0\psi(0)\,|\Omega\rangle \\
&= -\langle\Omega|\, \bar{\psi}(t)\gamma_0\Gamma_t^\dagger\gamma_0 Q(t)\bar{Q}(0)\Gamma_0\psi(0)\,|\Omega\rangle \\
&= -e^{-Mt}\left\langle \bar{\psi}(t)\gamma_0\Gamma_t^\dagger\gamma_0 U(t,0)\frac{1}{2}(\mathbb{1}+\gamma_0)\Gamma_0\psi(0)\right\rangle \\
&= -\frac{1}{2}e^{-Mt}\left\langle Tr[U(t,0)\gamma_0\Gamma_t^\dagger\gamma_0(\mathbb{1}+\gamma_0)\Gamma_0 D^{-1}(0,t)]\right\rangle
\end{aligned} \tag{A.9}$$

A.2.2 Pion correlator

The pion is the lightest meson consisting of a u- and a $\bar{d}$-Quark. The operator for a charged pion is the following:

$$\mathcal{O} = \sum_{\mathbf{x}} \bar{u}(x)\gamma_5 d(x) \tag{A.10}$$

The corresponding correlation function reads as follows

$$\begin{aligned}
C &= \langle\Omega|\, \mathcal{O}^\dagger(x_0)\mathcal{O}(y_0)\,|\Omega\rangle \\
&= \langle\Omega|\left(\sum_{\mathbf{x}} \bar{u}(x)\gamma_5 d(x)\right)^\dagger \sum_{\mathbf{y}} \bar{u}(y)\gamma_5 d(y)\,|\Omega\rangle \\
&= -\langle\Omega|\sum_{\mathbf{x}} \bar{d}(x)\gamma_5 u(x) \sum_{\mathbf{y}} \bar{u}(y)\gamma_5 d(y)\,|\Omega\rangle \\
&= -\langle\Omega|\sum_{\mathbf{x}} \bar{d}^a_A(x)(\gamma_5)_{AB} u^a_B(x) \sum_{\mathbf{y}} \bar{u}^b_C(y)(\gamma_5)_{CD} d^b_D(y)\,|\Omega\rangle \\
&= \langle\Omega|\sum_{\mathbf{x},\mathbf{y}} (\gamma_5)_{AB} u^a_B(x)\bar{u}^b_C(y)(\gamma_5)_{CD} d^b_D(y)\bar{d}^a_A(x)\,|\Omega\rangle \\
&= \sum_{\mathbf{x},\mathbf{y}} \left\langle (\gamma_5)_{AB} D^{-1(u)}(x,y)^{ab}_{BC}(\gamma_5)_{CD} \left(D^{-1(d)}(y,x)\right)^{ba}_{DA} \right\rangle \\
&= \sum_{\mathbf{x},\mathbf{y}} \left\langle (\gamma_5)_{AB} D^{-1(u)}(x,y)^{ab}_{BC}(\gamma_5)_{CD} \left(\gamma_5 D^{-1(d)\dagger}(x,y)\gamma_5\right)^{ba}_{DA} \right\rangle \\
&= \sum_{\mathbf{x},\mathbf{y}} \left\langle D^{-1(u)}(x,y)^{ab}_{BC} D^{-1(d)\dagger}(x,y)^{ba}_{DA} \right\rangle
\end{aligned} \tag{A.11}$$

If we apply the one-end trick, we end up with the following correlator:

$$C = \frac{1}{N}\sum_{n=1}^{N} \left\langle \sum_{\mathbf{x}} \phi^{(u)\dagger}[n,y_0](\mathbf{x},x_0)\phi^{(d)}[n,y_0](\mathbf{x},x_0) \right\rangle \tag{A.12}$$

References

[1] Christof Gattringer and Christian B Lang. *Quantum Chromodynamics on the Lattice: An Introductory Presentation*. Vol. 788. Lecture Notes in Physics. Springer, Berlin/Heidelberg, 2010. URL: http://physik.uni-graz.at/~lgt/qcdlatt/.

[2] J. Berlin. "Scalar tetraquark candidates on the lattice". PhD thesis. Goethe-Universität Frankfurt am Main, 2017.

[3] Andrea Shindler. "Twisted mass lattice QCD". In: 461.2-3 (May 2008), pp. 37–110. arXiv: 0707.4093 [hep-lat].

[4] Roberto Frezzotti et al. "Lattice QCD with a chirally twisted mass term". In: *arXiv e-prints* (Dec. 2000). arXiv: hep-lat/0101001.

[5] R. Frezzotti and G. C. Rossi. "Chirally improving Wilson fermions I. O(a) improvement". In: *Journal of High Energy Physics* (Aug. 2004). arXiv: hep-lat/0306014.

[6] A. Peters. "Investigation of heavy-light four-quark systems by means of Lattice QCD". PhD thesis. Goethe-Universität Frankfurt am Main, 2017.

[7] E. Eichten. "Heavy quarks on the lattice". In: *Nuclear Physics B - Proceedings Supplements* 4 (1988), pp. 170–177. ISSN: 0920-5632.

[8] Lowell S. Brown and William I. Weisberger. "Remarks on the static potential in quantum chromodynamics". In: *Phys. Rev. D* 20 (12 Dec. 1979), pp. 3239–3245.

[9] Pedro Bicudo et al. "Evidence for the existence of $ud\bar{b}\bar{b}$ and the nonexistence of $ss\bar{b}\bar{b}$ and $cc\bar{b}\bar{b}$ tetraquarks from lattice QCD". In: *prd* 92.1, 014507 (July 2015), p. 014507. arXiv: 1505.00613 [hep-lat].

[10] Pedro Bicudo et al. "B B interactions with static bottom quarks from lattice QCD". In: *prd* 93.3, 034501 (Feb. 2016), p. 034501. arXiv: 1510.03441 [hep-lat].

[11] Pedro Bicudo and Marc Wagner. "Lattice QCD signal for a bottom-bottom tetraquark". In: *prd* 87.11, 114511 (June 2013), p. 114511. arXiv: 1209.6274 [hep-ph].

[12] B. Blossier et al. "Efficient use of the Generalized Eigenvalue Problem". In: *arXiv e-prints* (Aug. 2008). arXiv: 0808.1017 [hep-lat].

[13] Karl Jansen and Carsten Urbach. "tmLQCD: A program suite to simulate Wilson twisted mass lattice QCD". In: *Computer Physics Communications* 180.12 (Dec. 2009), pp. 2717–2738. arXiv: 0905.3331 [hep-lat].

[14] C. Urbach et al. "HMC algorithm with multiple time scale integration and mass preconditioning". In: *Computer Physics Communications* 174.2 (Jan. 2006), pp. 87–98. arXiv: hep-lat/0506011 [hep-lat].

[15] Martin Lüscher. "A portable high-quality random number generator for lattice field theory simulations". In: *Computer Physics Communications* 79.1 (Feb. 1994), pp. 100–110. arXiv: hep-lat/9309020 [hep-lat].

[16] Marc Wagner. private notes/unpublished.

[17] Karl Jansen et al. "The static-light meson spectrum from twisted mass lattice QCD". In: *Journal of High Energy Physics* 2008.12, 058 (Dec. 2008), p. 058. arXiv: 0810.1843 [hep-lat].